



INSTITUT DE FRANCE
Académie des sciences

Comptes Rendus

Géoscience

Sciences de la Planète

Paola Stabile, Fabio Arzilli and Michael Robert Carroll

Crystallization of peralkaline rhyolitic magmas: pre- and syn-eruptive conditions of the Pantelleria system


Online first, 5th August 2021

[<https://doi.org/10.5802/crgeos.72>](https://doi.org/10.5802/crgeos.72)

Part of the Special Issue: Perspectives on alkaline magmas

Guest editor: Bruno Scaillet (Institut des Sciences de la Terre d'Orléans, CNRS, France)

© Académie des sciences, Paris and the authors, 2021.
Some rights reserved.

 This article is licensed under the
CREATIVE COMMONS ATTRIBUTION 4.0 INTERNATIONAL LICENSE.
<http://creativecommons.org/licenses/by/4.0/>



*Les Comptes Rendus. Géoscience — Sciences de la Planète sont membres du
Centre Mersenne pour l'édition scientifique ouverte
www.centre-mersenne.org*



Perspectives on alkaline magmas / *Perspectives sur les magmas alcalins*

Crystallization of peralkaline rhyolitic magmas: pre- and syn-eruptive conditions of the Pantelleria system

Paola Stabile^{*, a}, Fabio Arzilli^b and Michael Robert Carroll^a

^a School of Science and Technology, Geology Division, University of Camerino, Camerino, Italy

^b Department of Earth and Environmental Sciences, University of Manchester, Manchester, UK

E-mails: paola.stabile@unicam.it (P. Stabile), fabio.arzilli@manchester.ac.uk (F. Arzilli), michael.carroll@unicam.it (M. R. Carroll)

Abstract. Pantelleritic magmas are low-viscosity peralkaline rhyolites which exhibit large differences in eruptive style (explosive to effusive). The processes that promote fragmentation and explosive eruptions of pantelleritic magma remain subject to debate, but undoubtedly variations of magma viscosity during magma ascent and degassing contribute to differences in eruptive style. Because crystallization can significantly influence magma rheology, we present a review of equilibrium and disequilibrium crystallization experiments of pantellerites, focusing on the crystallization of the main phases, alkali feldspar, and (lesser) clinopyroxene. Our analysis of data for several explosive pantelleritic eruptions on Pantelleria suggests pre-eruptive pressures of 50–100 MPa, temperatures of 700–800 °C for water-saturated conditions. Given these conditions, we show that the low pre-eruptive crystal fractions (0.08 to 0.15), temperatures between 700 and 800 °C, and the decrease of melt H₂O content during magma ascent/decompression can promote a significant change in viscosity (up to 10⁶–10⁷ Pa·s), leading to magma brittle fragmentation and explosive eruptions. Because of their typical range of viscosity, pantelleritic magmas may show greater variations in eruptive style due to differences in ascent (decompression) rate when compared with metaluminous rhyolites.

Keywords. Alkaline magmas, Alkali feldspar, Clinopyroxene, Crystallization kinetics, Eruptive conditions, Eruptive dynamics.

Online first, 5th August 2021

1. Introduction

Pantellerites are typically identified as silica-oversaturated rhyolites with an alkali/alumina molar

ratio $[(\text{Na}_2\text{O} + \text{K}_2\text{O})/\text{Al}_2\text{O}_3]$ (Peralkalinity Index, P. I.) higher than the unity, and they are rich in Na with an excess of Fe over Al [see the trend in MacDonald, 1974, Le Maitre, 2002, Jordan et al., 2021]. They are often associated with comendites, with slightly lower SiO₂ and P.I. [e.g., Scaillet and MacDonald, 2003]. Both occur mainly in interplate settings, including

* Corresponding author.

oceanic islands [Ascension Island; e.g., Jeffery and Gertisser, 2018] to continental rift zones, as for example the Sicily channel rift zone [Pantelleria Island; White *et al.*, 2009], the Kenyan [e.g., Ren *et al.*, 2006, MacDonald *et al.*, 2011] and Ethiopian [e.g., Ronga *et al.*, 2009, Iddon *et al.*, 2018] Rift Valleys, and Mayor Island [NZ-Taupo Volcanic Zone; Barclay *et al.*, 1996].

Peralkaline rhyolites have lower viscosity than calcalkaline rhyolites due to the high alkali content that strongly depolymerizes the melt structure [Stevenson *et al.*, 1998, Mysen, 2007, Mysen and Toplis, 2007, Di Genova *et al.*, 2013, 2017, Stabile *et al.*, 2016, 2017, 2021], and they can shift between explosive and effusive eruptive behaviour, thus producing a wide variety of eruptive styles, ranging from lava flows and fountains to Strombolian to sub-Plinian and Plinian eruptions [e.g., Schmincke, 1974, Mahood and Hildreth, 1986, Duffield, 1990, Lowestern and Mahood, 1991, Houghton *et al.*, 1992, Stevenson *et al.*, 1993, Webster *et al.*, 1993, Wilding *et al.*, 1993, Barclay *et al.*, 1996, Stevenson and Wilson, 1997, Horn and Smincke, 2000, Gottsmann and Dingwell, 2002]. Although peralkaline rhyolites were once thought to be relatively H₂O poor [Bailey and MacDonald, 1987], more recent studies indicate magma water contents as high as 5–6 wt% H₂O [e.g., Kovalenko *et al.*, 1988, Webster *et al.*, 1993, Wilding *et al.*, 1993, Barclay *et al.*, 1996, Gioncada and Landi, 2010, Di Carlo *et al.*, 2010, Lanzo *et al.*, 2013, Romano *et al.*, 2019].

Pre-eruptive magmatic volatile contents and pre- and syn-eruptive crystallization and degassing can strongly affect the rheology of magma in the chamber and during magma ascent, and in turn, they can influence the volcanic eruptive styles of magmas. Many variables, including melt composition, crystallinity, temperature (T), pressure (P), undercooling ($\Delta T = T_{\text{liquidus}} - T_{\text{subliquidus}}$), time, melt water content, oxygen fugacity ($f\text{O}_2$), and cooling and decompression rates, can influence magma crystallization at depth and during ascent to surface [e.g., Couch *et al.*, 2003, Martel and Schmidt, 2003, Hammer, 2006, Brugger and Hammer, 2010, Mollard *et al.*, 2012, Martel, 2012, Shea and Hammer, 2013, Arzilli and Carroll, 2013, Arzilli *et al.*, 2016]. Crystallization has commonly been investigated in pantelleritic melts under equilibrium conditions [Scaillet and MacDonald, 2001, 2003, 2006, Di Carlo *et al.*, 2010, Romano *et al.*, 2020], but disequilibrium crystallization kinetics

deserve additional attention because of possible consequences for conduit flow processes and eruptive dynamics of peralkaline magmas [Arzilli *et al.*, 2020].

In this review, we provide a comprehensive evaluation of the pre-eruptive conditions of volcanic activities at Pantelleria, which have implications for rheological and numerical eruption models that investigate magma ascent and fragmentation of peralkaline rhyolitic magmas. The aim of this contribution is to understand the eruptive dynamics of pantelleritic magmas by studying the phase abundances and chemical compositions of the main mineralogical phases (i.e., alkali feldspar (Afs) and clinopyroxene (Cpx)) present in natural products of the Pantelleria volcanic system. Here, we focus our attention on equilibrium and disequilibrium crystallization of alkali feldspar and clinopyroxene in different experimental and natural pantelleritic products, from Strombolian eruptions of Cuddia del Gallo/Randazzo and Fastuca pantellerite and the Green Tuff Plinian eruption, with the aim of constraining the pre- and syn-eruptive conditions of these eruptions. Specifically, we investigate how different parameters, such as pre-eruptive temperature and crystal fraction of the main mineralogical phases and $(\text{H}_2\text{O})_{\text{melt}}$ (= concentration of H₂O dissolved in melt) influence the eruptive style of pantelleritic magma, contributing to reach magma fragmentation and promoting explosive eruptive behaviour.

2. Pantelleria volcanic system

Pantelleria Island is located in the Mediterranean Sea south of Sicily (Italy) within the Sicily Channel Rift Zone [Rotolo *et al.*, 2007, Civile *et al.*, 2008]. The volcanic island of Pantelleria is composed of “La Vecchia” caldera (114 ka) and the “Cinque Denti” [45.7 ± 1.0 ka; Scaillet *et al.*, 2013, Liszewska *et al.*, 2018], which suggest the presence of magma beneath the central area of the island [Civetta *et al.*, 1984, Mahood and Hildreth, 1986, Rotolo *et al.*, 2013, 2017]. Pantelleria has a bimodal magmatism association of transitional to alkali basalts, located mostly in the north-west sector of the island [Civetta *et al.*, 1988, Rotolo *et al.*, 2007], and trachytes-pantellerites which are more wide spread [e.g., Mahood and Hildreth, 1986, Civetta *et al.*, 1998, White *et al.*, 2005, 2009, Liszewska

et al., 2018, Scaillet *et al.*, 2011, 2013, Williams *et al.*, 2014, Jordan *et al.*, 2018, Rotolo *et al.*, 2021]. There is a clear compositional gap (Daly gap) between alkali basalt and peralkaline rhyolite end-members. Two main hypotheses have been proposed on the origin of the rhyolitic magmas: (i) low-degree partial melting of mafic cumulates in the lower crust to form trachyte, followed by crystal fractionation in shallow reservoirs to generate the most evolved pantellerites [Lowestern and Mahood, 1991, Bohrsen and Reid, 1997, Avanzinelli, 2004, MacDonald *et al.*, 2008, 2011, Marshall *et al.*, 2009]; (ii) fractional crystallization from an alkali basaltic parental magma [Civetta *et al.*, 1998, White *et al.*, 2005, 2009, Neave *et al.*, 2012, Romano *et al.*, 2019, 2020]. Rocks of intermediate compositions (such as mugearite and benmoreite) are rare and, in many cases, are thought to be the result of magma mixing based on textural observations [Romengo *et al.*, 2012, Liszewska *et al.*, 2018]; their rare eruption may represent a physical (density, viscosity) discrimination in the magma reservoirs [Civetta *et al.*, 1988, White *et al.*, 2009, Neave *et al.*, 2012, Liszewska *et al.*, 2018]. For instance, according to this last hypothesis, the Daly gap in Pantelleria compositions can be explained by the fact that the intermediate melts are not erupted because felsic magmas (trachytic to pantelleritic) within the magma chamber behave as a density filter for high-viscosity and crystal-rich intermediate magmas [Mungall and Martin, 1995, Peccerillo *et al.*, 2003]. Moreover, Prosperini *et al.* [2000] proposed a process of mixing plus fractional crystallization between the less evolved comenditic trachyte and the more evolved pantelleritic sample. This magmatic interaction process has been specifically considered the force triggering the magmatic events that produced the Khaggiar lava dome [6–8 ka; Speranza *et al.*, 2010, Scaillet *et al.*, 2011], which was followed by intense volcanic activity, characterized by explosive eruptions and lava flows emissions from different effusive centres [Civetta *et al.*, 1998, Orsi *et al.*, 1991, Scaillet *et al.*, 2011, Neave, 2020].

There exist many debates on pantelleritic magma genesis and their evolution and eruptive behaviour [e.g., see Romano *et al.*, 2018, 2020, and references therein]. Outcrops in Pantelleria show fall units (pumice fall, welded fall (splat-ter), etc.) and deposits of pantelleritic magmas,

which were originated from lava fountains, with a continuous transition from explosive to more effusive style [e.g., Jordan *et al.*, 2018]. An important question remains as to the mechanisms and processes triggering this shift in eruptive style for magmas with almost identical compositions [Schmincke, 1974, Duffield, 1990, Houghton *et al.*, 1992, Stevenson *et al.*, 1993, Webster *et al.*, 1993, Wilding *et al.*, 1993, Barclay *et al.*, 1996, Stevenson and Wilson, 1997, Horn and Smincke, 2000, Gottsmann and Dingwell, 2002, Hughes *et al.*, 2017].

For instance, it is well-known [e.g., Sparks, 1978, Papale and Polacci, 1999] that the increase in magma viscosity due to volatile loss can produce the conditions necessary for magma fragmentation and explosive eruptions [Di Genova *et al.*, 2013]. However, given the low viscosity of pantelleritic liquids [Neave *et al.*, 2012], there should be other mechanisms, which trigger the most explosive style. Previous studies have demonstrated that these peralkaline rhyolites, at low temperatures, have lower viscosity than metaluminous rhyolites due to the effect of alkalis that strongly depolymerize the melt, decreasing their configurational entropy and the viscosity [Di Genova *et al.*, 2013, 2017, Stabile *et al.*, 2016, 2017, 2021].

Viscosity effects on the eruption of pantelleritic magmas are further modelled and discussed by Campagnola *et al.* [2016], who presented numerical simulations on the conduit dynamics of the highly explosive Green Tuff eruption, the most recent catastrophic eruption on Pantelleria Island [Mahood and Hildreth, 1986, Williams, 2010, Williams *et al.*, 2014, Jordan *et al.*, 2018, 2021, Rotolo *et al.*, 2021]. The petrological data and the thermodynamic and numerical modelling indicate that pre-eruptive temperatures of the Pantelleria volcanic system for several explosive eruptions could range between 950 °C (high end-member associated with trachytic magmas) and 720–680 °C (associated with pantelleritic magmas) [White *et al.*, 2005, Di Carlo *et al.*, 2010, Campagnola *et al.*, 2016, Liszewska *et al.*, 2018, Romano *et al.*, 2020].

In the following discussion, we attempt to provide a more refined picture of the most probable pre-eruptive conditions for the Pantelleria eruptions, with a particular focus on the resulting rheological implications and eruptive behaviour.

3. Review of equilibrium and disequilibrium experiments on peralkaline rhyolitic melts

3.1. H_2O solubility in peralkaline rhyolite melts

Phase equilibrium studies can constrain the storage conditions of the specific magma system investigated, providing information on the magma evolution and magma chamber state prior to eruption [Rutherford *et al.*, 1985, Geschwind and Rutherford, 1992, Gardner *et al.*, 1995, Rutherford and Devine, 1996, Barclay *et al.*, 1998, Cottrell *et al.*, 1999, Di Carlo *et al.*, 2010, Romano *et al.*, 2018].

In this work, we consider studies on the phase relations as function of pressure, temperature, and water content in pantelleritic compositions (Table 1). In particular, water abundance in rhyolitic magmas can influence magma physical properties and crystallization behaviour [e.g., Hammer, 2004, Gualda *et al.*, 2012] and in turn, rheological properties and eruptive styles [e.g., Roggensack *et al.*, 1997, Huppert and Woods, 2002, Sparks, 2003, Cashman, 2004, Aiuppa *et al.*, 2007, Edmonds *et al.*, 2008, Stock *et al.*, 2018, Stabile and Carroll, 2020]. Much effort has been devoted to study water solubility in different silicate melt compositions, but only a few studies document water abundance in strongly peralkaline rhyolites and Fe-rich pantelleritic compositions [e.g., Scaillet and MacDonald, 2001, Schmidt and Behrens, 2008, Di Carlo *et al.*, 2010, Stabile *et al.*, 2018, 2020, Romano *et al.*, 2021].

Figure 1a shows the general state of knowledge concerning water solubility in pantelleritic magmas under water-saturated conditions. In the figure, we show solubility calculations as a function of pressure—at 750 °C—for two similar pantellerite compositions [Di Carlo *et al.*, 2010, Arzilli *et al.*, 2020] with all plotted results obtained from the thermodynamic models of Papale *et al.* [2006], Moore *et al.* [1998], and Ghiorso and Gualda [2015]. Generally, the data reflect the well-known strong pressure dependence of water solubility, although we are aware that the Papale *et al.* [2006] model tends to slightly overestimate water solubility in such melt compositions, while Moore *et al.* [1998] better reproduces the solubility data [see Romano *et al.*, 2021]. Overall, the solubility data demonstrate that water loss from pantelleritic melts during ascent can alter the fluid-phase mass fraction produced, depending on initial magma

water content and dynamics of degassing (bubble nucleation, growth, coalescence), and possible eventual fragmentation (for explosive eruptions).

3.2. Liquidus curves of alkali feldspar and clinopyroxene

Previous petrological studies have worked to better define the T – P range and the redox conditions of comenditic to pantelleritic magmas [Scaillet and MacDonald, 2001, 2003, 2006, White *et al.*, 2005, 2009, Di Carlo *et al.*, 2010, Romano *et al.*, 2020], as well as their pre-eruptive water contents [e.g., Giocada and Landi, 2010, Neave *et al.*, 2012, Lanzo *et al.*, 2013, Romano *et al.*, 2019]. The best-estimate alkali feldspar and clinopyroxene liquidus curves for two pantelleritic melts are shown in Figure 1b at temperatures of 700–850 °C and $P(H_2O)$ of 25–150 MPa. The two melts differ slightly in composition, with slightly higher wt% concentrations of FeO and Na₂O for the melt composition used by Arzilli *et al.* [2020], as well as a small difference in the P.I. of 1.46 vs. 1.40 for the Di Carlo *et al.* [2010] study (see Table 1).

Di Carlo *et al.* [2010] studied the role of different intensive parameters (P , T , H_2O in the melt and fO_2 on crystal–liquid equilibria) in a Pantelleria rhyolite belonging to the Fastuca pumice fall eruptive unit. Phase equilibria show that clinopyroxene is the first liquidus phase, followed by alkali feldspar and then quartz (which is here not reported) over the entire range of T – H_2O_{melt} investigated by Di Carlo *et al.* [2010], with aenigmatite being stable at temperature ≤ 700 °C, at pressures ≤ 100 MPa. Slightly different results on the same composition have been found by Romano *et al.* [2020], where the mineralogical assemblage is dominated by alkali feldspar, with minor aenigmatite and clinopyroxene, but also fayalite, amphibole, and quartz occurring in minor amounts at lower temperatures. In particular, the crystallization of fayalite in peralkaline magmas depends on a combination of temperature, fO_2 , and melt peralkalinity (and SiO₂ activity) and for Fastuca it is limited to T between 690–750 °C, for suitable peralkalinity of melt and fO_2 [Romano *et al.*, 2020]. These small differences between Romano *et al.* [2020] and Di Carlo *et al.* [2010] results, despite the use of nominally identical starting materials, are most likely due to the high sensitivity of the phase stabilities to small variation of intensive parameters, as for instance, the slightly

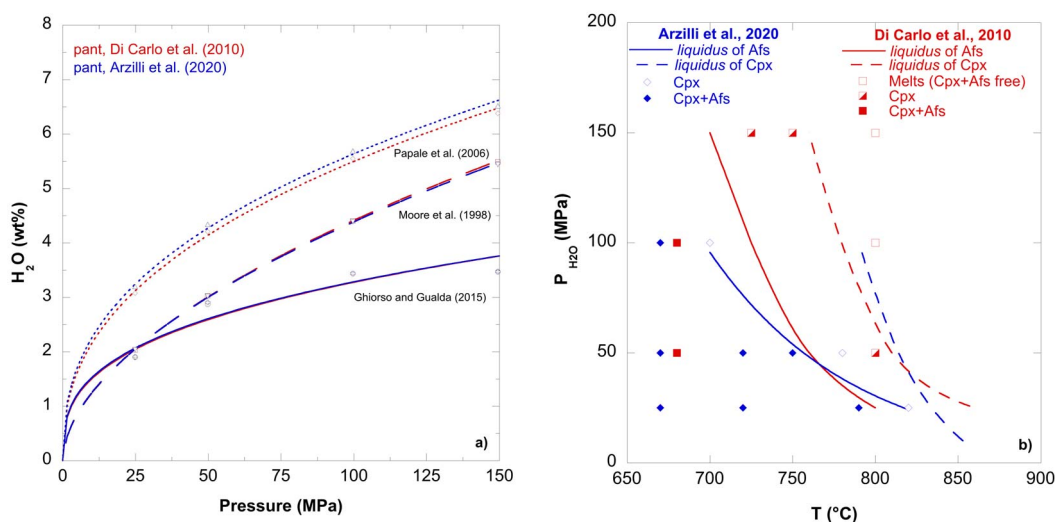


Figure 1. (a) Water content solubility calculations (at 750 °C) as function of pressure for pantelleritic compositions [Di Carlo et al., 2010, Arzilli et al., 2020] obtained by using Papale et al. [2006], Moore et al. [1998], and Ghiorso and Gualda [2015] solubility models. The purpose of the figure is to illustrate the H₂O-saturated conditions for the selected magma compositions for a given P – T range. See Romano et al. [2021] for more detailed discussion on water solubility in pantelleritic melts. (b) Phase diagram for alkali feldspar (Afs) and clinopyroxene (Cpx) under water-saturated conditions at NNO + 0.8 and NNO – 1,2 in pantelleritic compositions from Arzilli et al. [2020] and Di Carlo et al. [2010], respectively.

Table 1. Summary of pantelleritic data used in this study

(wt%)	Experimental data				Natural samples		
	Arzilli et al. [2020] Cuddia del Gallo	Di Carlo et al. [2010] Fastuca	Romano et al. [2020] Fastuca	Romano et al. [2020] Green Tuff	Rotolo et al. [2007] Fastuca (PAN0113)	Campagnola et al. [2016] Green Tuff	Gioncada and Landi [2010] Cuddia del Gallo (PANT15)
SiO ₂	69.13	70.40	69.45	72.60	69.98	69.4	66.3
TiO ₂	0.54	0.48	0.48	0.52	0.47	0.50	0.39
Al ₂ O ₃	10.46	10.30	10.15	9.00	9.75	8.40	10.28
Fe ₂ O ₃	n.a.	—	—	—	8.52	8.60	—
FeO*	8.06	7.52	7.87	6.24	—	8.41	—
MnO	0.30	0.26	0.21	0.24	0.27	0.30	0.29
MgO	0.09	0.06	0.10	0.51	0.00	0.10	0.05
CaO	0.56	0.52	0.53	0.46	0.55	0.40	0.43
Na ₂ O	6.30	5.67	6.71	7.29	7.02	6.30	6.10
K ₂ O	4.54	4.74	4.46	2.87	4.43	4.20	4.29
P ₂ O ₅	0.01	—	0.04	0.06	—	—	0.03
SO ₂	n.a.	—	—	—	—	—	—
F	n.a.	—	—	0.20	—	—	—
Cl	n.a.	—	—	—	—	—	—
Total	99.75	100.00	100.00	100.00	100.00	98.2	99.42
PI ¹	1.46	1.40	1.56	1.68	1.68	1.77	1.43

Notes: PI¹ (Peralkalinity Index) = molar (Na₂O + K₂O)/Al₂O₃. n.a. = not analysed.

lower redox conditions investigated in Romano *et al.* [2020] compared to Di Carlo *et al.* [2010]. However, in these evolved pantelleritic magmas, ferromagnesian phases are always limited to relatively small abundances and Afs, followed by Qz are the main phases to crystallize—these are all near-eutectic-type melts in which incompatible elements can vary widely in abundance, while major elements show only small variations.

In Figure 1b, we also report the liquidus temperatures of alkali feldspar obtained by Arzilli *et al.* [2020] and of clinopyroxene, using the composition of a peralkaline rhyolitic pumice (PANT15) from the eruptive fall unit of Cuddia del Gallo. These liquidii are consistent with those obtained from Di Carlo *et al.* [2010] at similar pressures, near water saturation. Although the oxygen fugacity of NNO +0.8 considered in Arzilli *et al.* [2020] is higher than those investigated (NNO – 1 to NNO – 2) by Di Carlo *et al.* [2010], the liquidii of the alkali feldspar are similar at pressures lower than 50 MPa (Figure 1b), which suggest that alkali feldspar is not strongly sensitive to fO_2 (which mainly influences melt FeO contents, and indirectly, SiO_2 activity). However, at pressures higher than 50 MPa, the alkali feldspar at NNO + 0.8 is stable at slightly lower temperatures compared with experiments at NNO – 1. This temperature difference at pressures higher than 50 MPa may be related to compositional difference between the two peralkaline rhyolitic melts (see Table 1). Moreover, reducing the redox conditions from NNO + 0.8 to NNO – 1.2 shifts the clinopyroxene liquidus at pressures higher than 50 MPa to lower temperatures (temperature difference of ~30 °C). On the other hand, the clinopyroxene liquidus from Di Carlo *et al.* [2010] shows broadly the same pattern than the alkali feldspar liquidus curve, but appearing at higher T (>750 °C). Overall, the relative order of crystallization of the main mineralogical phases is the same and persists over the P – T range for both melt compositions used by Di Carlo *et al.* [2010] and Arzilli *et al.* [2020].

3.3. Composition of alkali feldspar

The compositions of experimental alkali feldspars fall in the range of Or_{28–67} (Figure 2a). A broad negative correlation between Or (mol%) and T (°C) is evident when all the available data are plotted together (Figure 2a). For instance, for the pantellerites

in Arzilli *et al.* [2020], the Or content of alkali feldspar crystals formed at 670 °C ranges from 47 to 67 mol% (different melt H_2O), while the ones crystallized at temperatures ≥ 720 °C are characterized by a lower Or content between 31 and 37 mol% (near the binary Alb–Or minimum). Hence, the alkali feldspar is more sodic at temperatures between 720 and 790 °C, independent of P and H_2O dissolved in the melt [Arzilli *et al.*, 2020]. The grey shaded band in Figure 2a indicates the range of Or contents (between 34 and 38 mol%) in natural alkali feldspar crystals obtained from Cuddia del Gallo (PANT15), Fastuca and Green Tuff eruption products [Di Carlo *et al.*, 2010, Lanzo *et al.*, 2013, Liszewska *et al.*, 2018, Romano *et al.*, 2020]. The variation in Or content with temperature is appreciable only at ≤ 700 °C for experiments from Di Carlo *et al.* [2010] and Romano *et al.* [2020].

When we examine variations of Or content with H_2O_{melt} (Figure 2b), the majority of data displays limited variation with H_2O_{melt} except for the highest H_2O charges which appear to show a general positive correlation between Or and H_2O in the melt. However, when considering each subset of data relative to the melt compositions, which are reported from Di Carlo *et al.* [2010], Or defines a slight positive correlation with H_2O only for $H_2O > 2.5$ wt% at 100–150 MPa. Whereas an almost horizontal trend is obtained at lower H_2O contents for compositions falling in the range Or_{28–39}. Overall, the composition of natural alkali feldspar in pantellerites is well reproduced at 720–750 °C and $(H_2O)_{\text{melt}}$ in the range 2.5–4 wt%. Higher or lower temperatures cannot reproduce the natural alkali feldspar composition (grey band in the figure).

3.4. Composition of clinopyroxene

Experimental clinopyroxenes have compositions in the range of X_{Fe} (=molar Fe/(Fe + Mg), with all Fe as Fe^{2+}) between 0.54 and 0.97 for data reported on GTP (Green Tuff Pantellerite) and FP (Fastuca Pantellerite) from Romano *et al.* [2020], while it varies between 0.84 and 0.99 for data on FP of Di Carlo *et al.* [2010] (Figure 3a).

X_{Fe} shows a negative correlation with temperature in the different pantelleritic products. In particular, at constant H_2O_{melt} , in GTP clinopyroxenes, a decrease in temperature of 50 °C (from 800 to 750 °C) increases X_{Fe} from 0.60 to 0.80, in FP, clinopyroxene

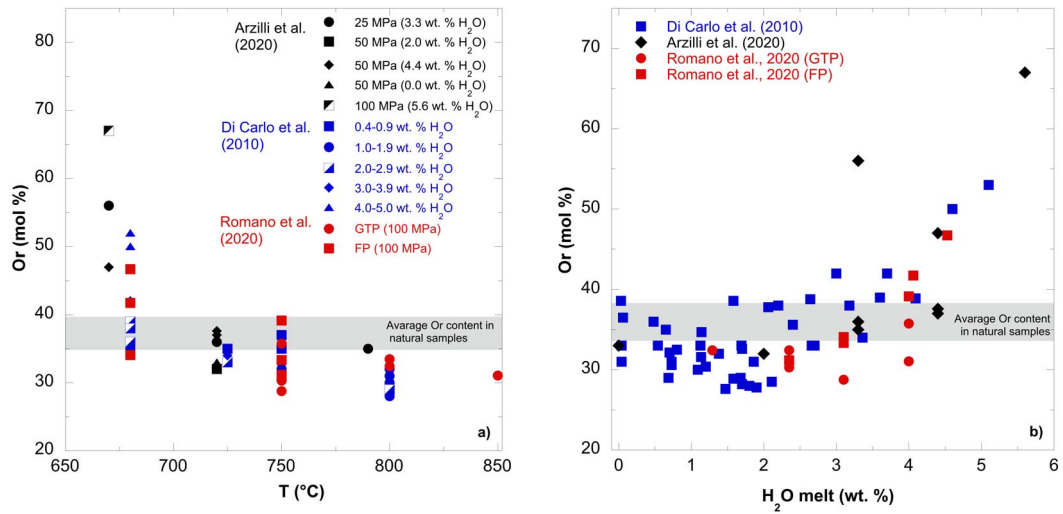


Figure 2. (a) Orthoclase (Or) mol% content of alkali feldspars as a function of experimental temperature (T °C) and (b) H_2O dissolved in the melt in pantelleritic compositions [Di Carlo *et al.*, 2010, Arzilli *et al.*, 2020, Romano *et al.*, 2020]; the total P range considered is between 50 and 150 MPa. GTP in the legend indicates Green Tuff pantellerite, while FP is Fastuca pantellerite [Romano *et al.*, 2020]. The grey shaded band indicates the range of Or contents (34–38 mol%) in natural alkali feldspar phenocrysts [Lanzo *et al.*, 2013].

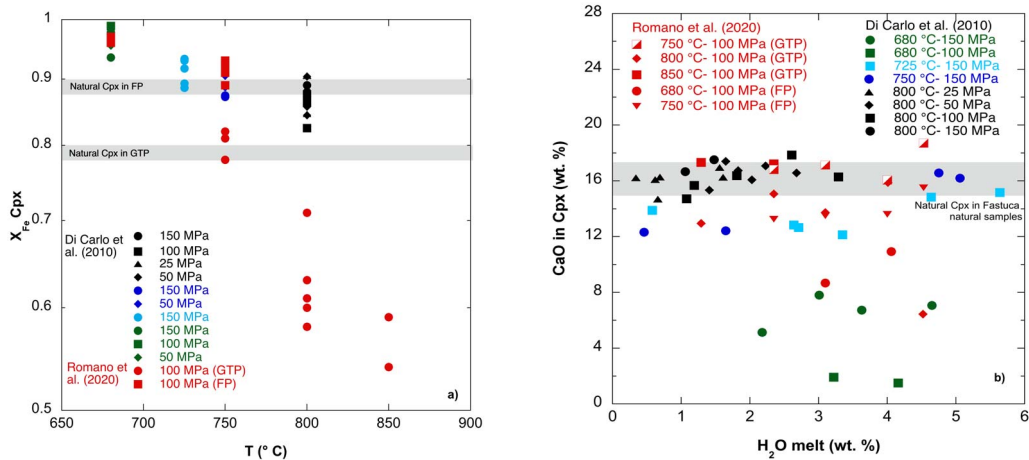


Figure 3. (a) Variation of X_{Fe} ($=FeO^*/(FeO^* + MgO)$ molar), where FeO^* is total iron expressed as FeO of experimental Cpx, with Temperature (°C) at a range of pressures [Di Carlo *et al.*, 2010, Romano *et al.*, 2020]. The grey bands correspond to the natural compositions of Cpx (GTP = Green Tuff Pantellerite; FP = Fastuca Pantellerite). (b) Variation of CaO content (wt%) of experimental Cpx with melt water content (H_2O_{melt} wt%) at a range of temperatures and pressures [Di Carlo *et al.*, 2010, Romano *et al.*, 2020]. The grey band corresponds to the average CaO content of Cpx phenocrysts in the starting rocks (Fastuca and Green Tuff Pantellerite).

only crystallizes at lower temperature ($<800\text{ }^{\circ}\text{C}$), and the X_{Fe} ranges from 0.89 to 0.97. The most Fe-rich clinopyroxene crystals are produced at $680\text{ }^{\circ}\text{C}$ in FP compositions [Romano *et al.*, 2020]. Similarly, experimental data from Di Carlo *et al.* [2010] display the highest X_{Fe} values (between 0.92 and 0.99) at the lowest temperature investigated of $680\text{ }^{\circ}\text{C}$. Clinopyroxene compositions synthesized at $750\text{ }^{\circ}\text{C}$ reproduce the small range of natural clinopyroxene compositions [Romano *et al.*, 2020], while clinopyroxenes obtained by Di Carlo *et al.* [2010] at temperatures between 720 and $800\text{ }^{\circ}\text{C}$ better reproduce the natural clinopyroxene compositions of Fastuca products (upper grey band in Figure 3a).

3.5. Crystallization of alkali feldspar and clinopyroxene

Although the crystallization behaviour of peralkaline rhyolites is relatively well-understood at equilibrium, the prediction of the crystallization kinetics under non-equilibrium, time-dependent conditions is still difficult, even though kinetic data can potentially provide new insights about the timescales of the magmatic processes. Here, we summarize the current understanding of the crystallization kinetics of alkali feldspar and clinopyroxene under both equilibrium and disequilibrium conditions in pantelleritic magma compositions. Alkali feldspars are highly sensitive to variations of intensive variables in volcanic systems, which are recorded by variable textures and compositional zoning patterns, depending on the rate of change of intensive parameters promoting crystallization. Recently, several studies have investigated clinopyroxene crystallization in different alkaline magma because clinopyroxene crystallization can also rapidly change the magma rheology, and chemical zoning of clinopyroxene can provide information on the magma history [e.g., Ni *et al.*, 2014, Polacci *et al.*, 2018, Masotta *et al.*, 2020, Pontesilli *et al.*, 2019, Arzilli *et al.*, 2019]. Here, we report the total crystal fraction (ϕ_{total}), which represents the sum of both alkali feldspar and clinopyroxene crystal fraction, in experimental runs on pantellerites from Cuddia del Gallo, Fastuca, and Green Tuff [Di Carlo *et al.*, 2010, Arzilli *et al.*, 2020, Romano *et al.*, 2020] as function of ΔT_{Cpx} (temperature below the clinopyroxene liquidus).

Results show ϕ_{total} between 0.08 and 0.29 for ΔT_{Cpx} between 10 and $140\text{ }^{\circ}\text{C}$ and $(\text{H}_2\text{O})_{\text{melt}}$ in the range of 3.3–5.6 wt% for Arzilli *et al.* [2020] [consistent with melt inclusion water content estimations in phenocrysts; Gioncada and Landi, 2010]. Considering both experimental data from Di Carlo *et al.* [2010] and Romano *et al.* [2020], ϕ_{total} (clinopyroxene + alkali feldspar phenocrysts) ranges between 0.01 and 0.49 for ΔT_{Cpx} up to $\sim 170\text{ }^{\circ}\text{C}$. The phase abundances along with the total crystal fraction (ϕ) for the investigated experimental conditions in Arzilli *et al.* [2020] are also reported in Table 2. The experimental durations vary between 24 and 288 h [Arzilli *et al.*, 2020] and demonstrate long nucleation delay of alkali feldspar in pantelleritic melts (from several hours to several days). The nucleation delay of alkali feldspar under water-undersaturated conditions can be ~ 230 h, and the nucleation delay time decreases with increasing melt H_2O content at fixed P and/or ΔT . Particularly, under water-saturated conditions, the nucleation delay of alkali feldspar is <50 h, while the nucleation delay of clinopyroxene ranges from minutes to a few hours [Arzilli *et al.*, 2020]. This indicates that clinopyroxene formation timescales can be significantly shorter than timescales for alkali feldspar formation upon changes of magmatic P – T conditions in pantelleritic magmas. Slow feldspar crystallization/recrystallization time scales are also observed in plagioclase-bearing basaltic magmas [Polacci *et al.*, 2018, Masotta *et al.*, 2020, Pontesilli *et al.*, 2019]. Importantly, we observe that despite a wide range of ΔT , the variation of clinopyroxene crystal fraction is relatively small from 0.02 to 0.10 [Di Carlo *et al.*, 2010, Romano *et al.*, 2020]. This implies that peralkaline rhyolites may spend days in sub-liquidus conditions without experiencing significant changes in crystal fraction due to long nucleation delay times for alkali feldspar [discussed in more detail in Arzilli *et al.* [2020]].

4. Discussion

4.1. Pre-eruptive conditions of the Pantelleria volcanic system

4.1.1. Strombolian eruptions

The strombolian pantelleritic products of Fastuca, Cuddia Randazzo, and Cuddia del Gallo have a

Table 2. Experimental run conditions and phase abundances for the data reported in Arzilli *et al.* [2020]

Sample	Pressure (MPa)	Temperature (°C)	H ₂ O (wt%)	<i>t</i> (h)	Phase abundances (wt%)	Total Φ
C136	100	670	5.6	192	Gl(83), Afs(7), Cpx(10), Ox(<1)	0.17
C144	50	750	4.4	288	Gl(92), Afs(6), Cpx(2)	0.08
C155	50	720	4.4	96	Gl(89), Afs(7), Cpx(3), Ox(1)	0.11
C148	50	720	4.4	175	Gl(85), Afs(8), Cpx(6), Ox(1)	0.15
C149	50	720	4.4	195	Gl(83), Afs(10), Cpx(6), Ox(1)	0.17
C141	50	670	4.4	72	Gl(71), Afs(20), Cpx(9)	0.29
C146	25	790	3.3	288	Gl(83), Afs(12), Cpx(3), Ox(2)	0.17
C151	25	720	3.3	130	Gl(75), Afs(19), Cpx(5), Ox(1)	0.25
C138	25	670	3.3	24	Gl(90), Afs(2), Cpx(8), Ox(<1)	0.10

Gl = glass; Afs = Alkali feldspar; Cpx = Clinopyroxene; Ox = oxides (Magnetite–Ülvöspinel solid solution, Fe–Ti oxides). Phase abundances calculated by multiple linear regression using known starting composition and crystal compositions analysed by microprobe; total Φ means total crystal fraction (% crystals/100).

mineral assemblage that consists of alkali feldspar, clinopyroxene, and minor amounts of fayalite, aenigmatite, amphibole, and quartz [Di Carlo *et al.*, 2010, Gioncada and Landi, 2010, Lanzo *et al.*, 2013, Landi and Rotolo, 2015, Romano *et al.*, 2020]. Alkali feldspar is the dominant crystal phase, and together with clinopyroxenes, occurs as both phenocrysts (between 500 μm to mm sizes) and microlites (from a few microns to 100–200 μm) [Di Carlo *et al.*, 2010, Gioncada and Landi, 2010, Romano *et al.*, 2020]. The abundance of phenocrysts is similar among the strombolian products of Fastuca, Cuddia del Gallo, and Cuddia Randazzo. The phenocrysts crystal fraction is ~ 0.15 (alkali feldspar + clinopyroxene). Fastuca samples also contain alkali feldspar phenocrysts, and alkali feldspar and clinopyroxene microlites [Romano *et al.*, 2020]. Similarly, alkali feldspar microlites are present within the ground-mass of the Cuddia Randazzo products. For most of the samples, the abundance of alkali feldspar microlites ranges between 0.56 and 0.66 of total crystals, while mafic mineral crystal fractions are ~ 0.05 – 0.11 [Landi and Rotolo, 2015]. Experimental temperatures between 720 and 800 °C and pressures of 25–100 MPa produce crystal fractions (~ 0.15 ; considering alkali feldspar + clinopyroxene) similar to the phenocryst abundances observed in the strombolian products of Fastuca, Cuddia Randazzo, and Cuddia del Gallo. Experiments also indicate that a crystal fraction of ~ 0.50 can be produced at

temperatures between 680 and 750 °C (Figure 4). Therefore, abundant microlites may be produced within this range of temperature in the strombolian eruptions.

Regarding the Fastuca strombolian eruption, equilibrium experiments indicate that the composition of natural clinopyroxene phenocrysts ($X_{\text{Fe}} = 0.88$ – 0.90) can be reproduced at temperatures between 725 and 800 °C and pressures between 25 and 150 MPa (Figure 3a). Instead, the compositions of natural alkali feldspar phenocrysts are reproduced at temperature between 680 and 750 °C, pressures between 50 and 100 MPa (Figure 2a), and water contents between 2 and 3.5 wt%. These results indicate that there is a narrow temperature window, between 725 and 750 °C, in which clinopyroxene and alkali feldspar can crystallize at the same conditions. This implies that either pre-eruptive temperatures of Fastuca eruption were between 725 and 750 °C or that magma was cooled down in a magma reservoir or during magma ascent from 800 °C to temperatures at which alkali feldspar can crystallize (680–750 °C). Furthermore, the rare occurrence of amphibole in Pantelleria rhyolites [Jordan *et al.*, 2018, Rotolo *et al.*, 2007, White *et al.*, 2009] suggests that this mineral crystallizes from a wetter and cooler magma storage region [Di Carlo *et al.*, 2010]. In this way, amphibole and alkali feldspar would coexist at $T > 680$ °C for crystal contents comparable with those observed in natural pantellerite [Romano *et al.*, 2020].

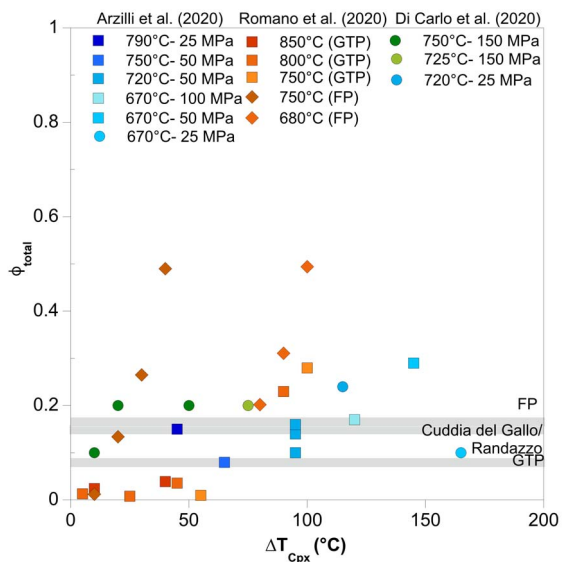


Figure 4. Total crystal fraction (Φ) of Afs + Cpx as function of ΔT_{Cpx} ($^{\circ}\text{C}$ below estimated Cpx liquidus temperature). The diagram shows data for peralkaline rhyolites from Di Carlo *et al.* [2010], Arzilli *et al.* [2020], and Romano *et al.* [2020] and data of total Φ of main eruptive pantellerite products [i.e., Fastuca, Cuddia del Gallo, Green Tuff; Gioncada and Landi, 2010, Lanzo *et al.*, 2013, Landi and Rotolo, 2015]. See text for discussion of ΔT_{Cpx} .

Eruptive temperatures $\geq 800^{\circ}\text{C}$, as we have demonstrated in Figures 2, 3 and 4 are not consistent with observations on crystal compositions and abundances of alkali feldspar and clinopyroxene for the different strombolian products considered here (Fastuca, Cuddia Randazzo and Cuddia del Gallo). This is also supported by the presence of aenigmatite, which is only stable at temperature of 750°C and 50 MPa for dry conditions and 750°C , 100 MPa, and wet conditions, as reported from Di Carlo *et al.* [2010] and Romano *et al.* [2020], respectively.

Considering the total crystal abundance of alkali feldspar and clinopyroxene (phenocrysts and microlites) in the strombolian products and the compositions of alkali feldspar and clinopyroxene phenocrysts observed in Fastuca eruptive products, we propose that the more likely pre-eruption conditions are $680\text{--}750^{\circ}\text{C}$, 25–100 MPa under water-saturated (or near-saturated) conditions.

4.1.2. Plinian eruption

The Green Tuff Plinian eruption produced an ignimbritic deposit that is compositionally zoned, from pantelleritic at the base to comenditic trachyte at the top of the deposit. This suggests that the magma reservoir of the Green Tuff was also compositionally zoned before the eruption: pantelleritic magma at the top and comenditic trachyte at the bottom of the reservoir [Liszewska *et al.*, 2018].

The mineral assemblage of the pantelleritic magma consists mainly of alkali feldspar, with minor clinopyroxene and aenigmatite, and traces of fayalite and quartz. Alkali feldspar represents the main crystal phase (>85 vol.%) of the phenocryst assemblage in every sample [White *et al.*, 2009]. Microlites are not present within the Green Tuff pantelleritic products [Campagnola *et al.*, 2016]. The textures of pantelleritic pumices erupted from Green Tuff Plinian eruption are mainly vitrophyric and crystal fraction of phenocrysts ranges between 0.05 and 0.25 [White *et al.*, 2009, Lanzo *et al.*, 2013, Campagnola *et al.*, 2016, Liszewska *et al.*, 2018, Romano *et al.*, 2019]. Although the observed crystal fraction covers a broad range, observations on numerous natural samples, suggest an average crystal fraction of 0.08 is representative for the pantelleritic member, with the later trachytic part of the eruption being more crystal-rich compared with the earlier pantelleritic part [Campagnola *et al.*, 2016]. The mineral assemblage of the trachytic member of the Green Tuff eruption consists of alkali feldspar and clinopyroxene, with minor olivine, ilmenite, and apatite [Campagnola *et al.*, 2016, Liszewska *et al.*, 2018, Romano *et al.*, 2020]. Both phenocrysts and microlites are present in the trachytic magmas. Alkali feldspar is the main phase (phenocrysts = 0.18 (%vol); microlites = 0.05), whilst, clinopyroxene is the second main phase in terms of crystal abundance (phenocrysts = 0.04; microlites = 0.06, according to Campagnola *et al.* [2016]).

Previous studies indicate that a thermal gradient was present within the magma reservoir at pre-eruptive conditions: the pantelleritic magma at the top was colder ($700\text{--}750^{\circ}\text{C}$) than the trachytic member ($900\text{--}950^{\circ}\text{C}$) in the lower part of the reservoir [Campagnola *et al.*, 2016, Liszewska *et al.*, 2018]. Water contents range from 1 wt% in the trachytes to 4 wt% in the pantellerites [Liszewska *et al.*, 2018]. Previous studies also estimated ~ 100 MPa as pre-

eruptive pressure, which correspond to depths of 3–4 km [Campagnola *et al.*, 2016, Liszewska *et al.*, 2018]. This depth is consistent with geophysical studies [e.g., Mattia *et al.*, 2007], which place the top of the magma reservoir at 4 km beneath the caldera. This implies that at ~100 MPa, and with 4 wt% of H₂O the pantelleritic magma was likely near water-saturated conditions (see Figure 1a) prior to eruption, particularly if we consider that the Papale *et al.* [2006] model may slightly overestimate H₂O solubility in pantelleritic magmas (as suggested by Romano *et al.* [2021]).

The composition of natural clinopyroxene phenocrysts ($X_{\text{Fe}} = 0.78\text{--}0.80$) of Green Tuff pantelleritic products can be reproduced experimentally at temperatures between 750 and 850 °C at ~100 MPa (Figure 4a,b), whereas the compositions of natural alkali feldspar are reproduced at temperature of 750 °C, 100 MPa, and 3–4 wt% of H₂O. Therefore, crystallization of the pantelleritic magma may occur near water-saturated condition before the Plinian eruption.

As we observed for the Fastuca products, clinopyroxene can crystallize at higher temperatures (750–850 °C) than alkali feldspar. However, the pre-eruptive temperatures of the Green Tuff pantelleritic products under water-saturated conditions cannot be higher than 750 °C, as the alkali feldspar is the main phase in terms of abundance. This is also confirmed by the experimental results of Romano *et al.* [2020], which show alkali feldspar is present only at temperatures ≤ 750 °C at 100 MPa and 4 wt% of H₂O, whereas at temperatures ≥ 800 °C alkali feldspar is not able to crystallize. This implies that either pre-eruptive temperature of the pantelleritic magma was at ~750 °C or that the magma cooled down in a magma reservoir from 850 °C to ~750 °C forming clinopyroxene first at higher temperatures and then alkali feldspar at lower temperatures, before the Plinian eruption was triggered; these scenarios should be further investigated, as they have implications on the triggering of the eruption and the eruption styles.

Experimental results suggest that at ΔT_{Cpx} between 3 and 170 °C and experimental duration between 24 and ~500 h, pantelleritic melts can produce crystal fractions (considering alkali feldspar and clinopyroxene) between 0.02 and ~0.50. Figure 5

shows calculated magma viscosities and crystal fractions for different melt water contents, at temperatures ranging from 700–850 °C (see figure legend for details). In general, low ΔT_{Cpx} (<75 °C) can promote a total crystal fraction similar to the natural pantelleritic products of Green Tuff Plinian eruption which are shown with green arrow in Figure 5 [Lanzo *et al.*, 2013, Campagnola *et al.*, 2016, Romano *et al.*, 2020]. For ΔT_{Cpx} higher than 75 °C, experimental crystal fractions are higher than those observed in the Green Tuff pantelleritic products. One condition in Figure 5 corresponding to $\Delta T_{\text{Cpx}} = 170$ °C (25 MPa, 670 °C) shows a ϕ_{total} of 0.10, which is similar to that of the Green Tuff pantelleritic products, but the ratio of clinopyroxene to alkali feldspar is too high and not representative of the natural samples. This is due to the combination of low temperatures (670 °C) the high ΔT_{Cpx} , which are not likely pre-eruptive conditions of Green Tuff Plinian eruption. Based on the chemical compositions of clinopyroxene and alkali feldspar, the likely pre-eruptive temperatures of the pantelleritic magma is ~750 °C (Figure 5b), which implies relatively small ΔT_{Cpx} (<75 °C). Small ΔT_{Cpx} may promote a nucleation delay of alkali feldspar crystals. Magma stagnation at small ΔT_{Cpx} for a few days prior to the triggering of the eruption may only produce a limited amount of crystallization. This indicates that although the pantelleritic member spends days rather than hours at sub-liquidus conditions, it may not produce drastic changes in (alkali feldspar) crystal fraction [Arzilli *et al.*, 2020]. Instead, the trachytic magma at the bottom of the reservoir is more crystallized than the pantelleritic member, as trachytic magmas can reach faster the equilibrium crystal fraction [Arzilli *et al.*, 2018, 2020]. The injection of hotter mafic-intermediate magma into the cooler reservoir destabilized the system, heating the trachytic magma (whose phenocrysts are partially resorbed but with no evidence of physical and chemical mixing) and triggering the Green Tuff eruption [Landi and Rotolo, 2015, Romano *et al.*, 2018, Liszewska *et al.*, 2018, Neave, 2020]. Thus, we propose that the Green Tuff pantelleritic magma was stored for days at pre-eruptive temperature of ~750 °C, pressure 100 MPa, and under near water-saturation conditions and was erupted suddenly after the injection of hotter magma into the reservoir without having time for significant changes in crystal volume fraction.

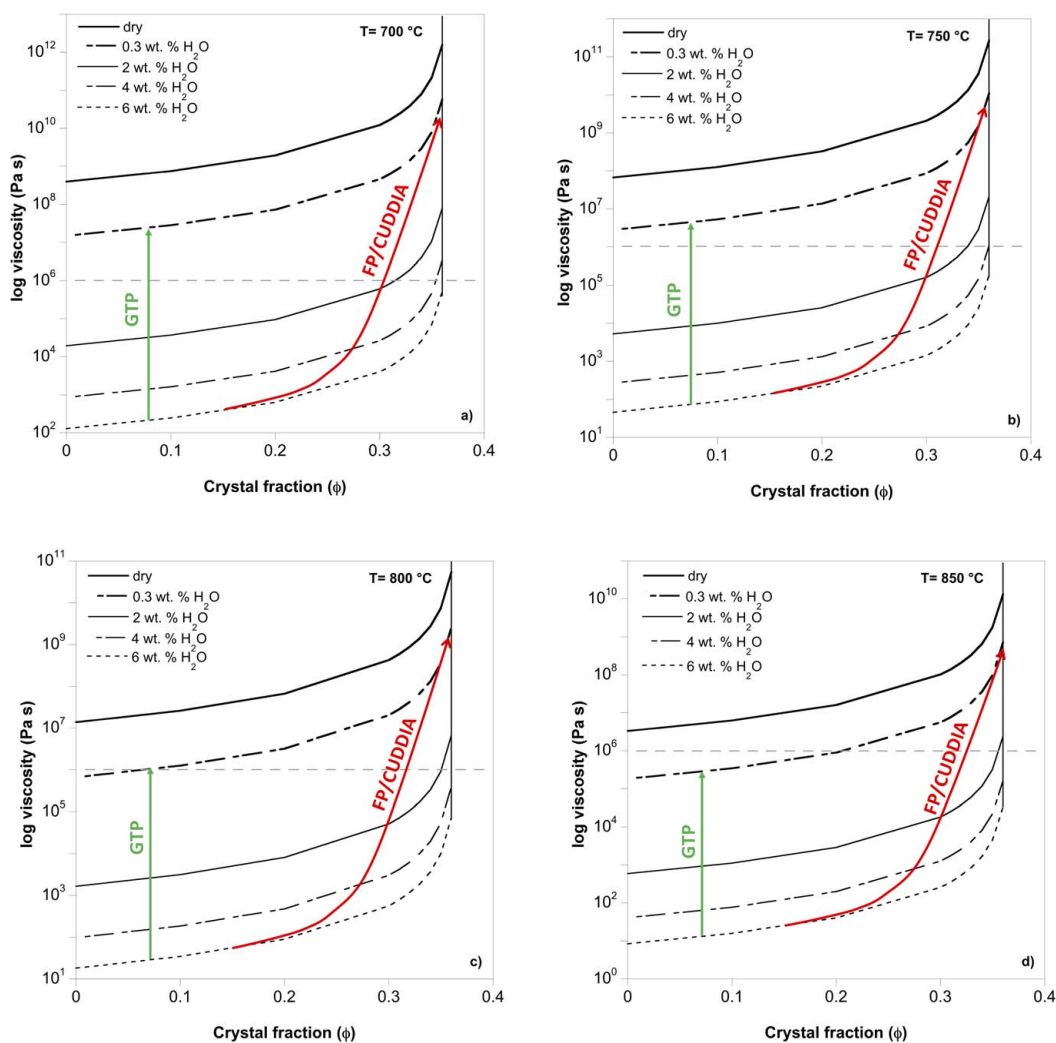


Figure 5. Effect of crystal content on liquid (magma) viscosity as function of water content (from dry conditions to 6 wt% H₂O) at different magmatic temperatures of (a) 700 °C, (b) 750 °C, (c) 800 °C, and (d) 850 °C. The arrows in the figures, starting from the natural phenocryst content (average) of the main eruptive products (Green Tuff or GTP, Cuddia del Gallo/Randazzo, Fastuca eruptions or FP/CUDDIA), indicate the different paths of rising magmas. The grey dashed line indicates the fragmentation level corresponding to a viscosity value of 10⁶ Pa·s. The viscosities of crystal-bearing and vesicle-free suspensions have been estimated by using the Mader et al. [2013] equations as function of crystal fraction, of a strain rate of $\dot{\gamma} = 1 \text{ s}^{-1}$, and a mean crystal aspect ratio of $r_p = 8$. See text for discussion.

In the following, we present and discuss the different effects of the initial temperature, H₂O_{melt}, crystal fraction, and crystal aspect ratio of alkali feldspar and clinopyroxene on the rheology and dynamics of the pantelleritic magma of the Pantelleria volcanic system.

4.2. Syn-eruptive conditions and rheological implications

Viscosity (η) calculations on dry and hydrous pantelleritic magma compositions (Cuddia del Gallo, Fastuca, and Green Tuff) can help understand better the

interactions between magma rheology and eruptive styles. Brittle magma fragmentation occurs when a critical viscosity-dependent strain rate is exceeded [Papale, 1999]. Melt composition, crystal fraction, and vesicularity all influence the bulk magma viscosity [e.g. Giordano *et al.*, 2008, Vona *et al.*, 2011, Mader *et al.*, 2013]. The bulk magma viscosity increases as the magma crystallinity increases and during degassing as magma water content decreases [e.g., Giordano *et al.*, 2008, Vona *et al.*, 2011]. This favours approaching brittle magma fragmentation conditions. Regarding peralkaline rhyolitic explosive eruptions, magma fragmentation still remains an unclear process [Di Genova *et al.*, 2013, Campagnola *et al.*, 2016, Hughes *et al.*, 2017].

For viscosity calculations, we consider the pre-eruptive temperatures of the Pantelleria volcanic system, the melt water content, the crystal fractions (ϕ), and the crystal aspect ratio (r_p). We use the model of Di Genova *et al.* [2013] for the prediction of the initial viscosity of peralkaline silicate melts as a function of temperature and water content. Assuming a pre- to syn-eruptive temperature of 700–850 °C, H_2O_{melt} between 0 and 6 wt%, and pressure of 25–100 MPa, we calculate the viscosities of pantelleritic liquids at this range conditions (Figure 5).

To investigate how the presence of crystals can influence the rheology of peralkaline rhyolitic magmas, the viscosities of crystal-bearing and vesicle-free suspensions have been estimated by using the Mader *et al.* [2013] equations using a strain rate of $\gamma = 1 \text{ s}^{-1}$ and a mean crystal aspect ratio of $r_p = 8$. For simplicity here, a strain rate of 1 s^{-1} has been considered assuming that the crystallization occurs at near-equilibrium conditions, while the crystal aspect ratio represents the average value between alkali feldspar and clinopyroxene obtained from crystallization experiments performed by Arzilli *et al.* [2020] under a wide range of ΔT_{Cpx} (3–170 °C). Viscosities are reported in Figure 5(a–d) as a function of the crystal fraction (alkali feldspar and clinopyroxene phenocrysts) for a given eruptive temperature (700–750–800–850 °C, Figure 5a–d) and H_2O_{melt} varying from 0 (dry conditions) up to 6 wt%. We consider 0.3 wt% of H_2O the residual water content at the exit of the vent, following the modelling of Green Tuff eruption [Campagnola *et al.*, 2016].

Overall, the viscosity increase is not linear with crystal fraction and it becomes steep for ϕ values

>0.35 , approaching infinite values for further ϕ increases [a consequence of the form of viscosity-crystal fraction relationship used by Mader *et al.* [2013]]. At a given temperature, the decrease of H_2O_{melt} during magma ascent can change the viscosity by up to 6 log units (Figure 5). At viscosities higher than $10^6 \text{ Pa}\cdot\text{s}$ (grey dashed line corresponding to the fragmentation level in Figure 5), brittle fragmentation may be invoked in agreement with modelling results obtained by Campagnola *et al.* [2016] and the rheological calculations reported by Hughes *et al.* [2017].

The pre-eruptive conditions of the strombolian cases (Fastuca, Cuddia Randazzo, and Cuddia del Gallo—red paths in Figure 5) can promote crystallization of phenocrysts and microlites of alkali feldspar and clinopyroxene at temperatures of 680–750 °C. The high total crystal fraction (phenocrysts and microlites) observed in the strombolian products may be produced during magma stagnation and slow ascent prior to the triggering of the eruption. As shown in Figure 5 large undercoolings and several days at pre-eruptive conditions are needed to produce high crystal fractions of alkali feldspar [Arzilli *et al.*, 2020]. The pre-eruptive conditions proposed for the strombolian eruptions and crystal abundance observed in the natural samples can increase viscosity during magma ascent (Figure 5a,b) at $\eta > 10^6 \text{ Pa}\cdot\text{s}$, which is sufficient to lead to brittle fragmentation.

Regarding the Green Tuff Plinian eruption (green paths in Figure 5), the pre-eruptive conditions of the crystal-poor pantelleritic member are likely a temperature of $\leq 750 \text{ °C}$, a pressure $\sim 100 \text{ MPa}$, and water-saturated conditions (in agreement with Campagnola *et al.* [2016] and Liszewska *et al.* [2018]). Despite the crystal content of the pantelleritic products being relatively low (on average 0.08), magma viscosity can reach values higher than $10^6 \text{ Pa}\cdot\text{s}$ close to the surface (0.3 wt% of H_2O) at temperatures $\leq 750 \text{ °C}$ (Figure 5a,b), which implies that brittle fragmentation may be promoted. At a temperature of 800 °C, magma viscosity can reach a value of $10^6 \text{ Pa}\cdot\text{s}$ only at the surface with a crystallinity of 0.08 (Figure 5c). At temperature of 850 °C this viscosity threshold is not reached (Figure 5d); therefore, it is unlikely that brittle fragmentation and explosive eruptions are promoted at temperatures $\geq 800 \text{ °C}$. This result is in agreement with previous studies [Campagnola *et al.*, 2016, Hughes *et al.*, 2017], however, our simple

model considers only the effect of crystals, temperature, and magma water content at the equilibrium conditions, whilst, the effect of decompression rate, adiabatic cooling ascent rate, strain rate, vesicularity, and outgassing during magma ascent should be considered [La Spina *et al.*, 2021]. For example, Hughes *et al.* [2017] suggest that bubble overpressure driven by rapid decompression and strain localization around crystals may also promote brittle magma fragmentation.

In conclusion, we note that crystal abundance does not play a fundamental role in changing the viscosity of the pantelleritic magma for the Green Tuff Plinian eruption, in agreement with Campagnola *et al.* [2016] and Hughes *et al.* [2017]. This contrasts with basaltic compositions, where fast syn-eruptive crystallization has been proposed as a driving mechanism triggering fragmentation and highly explosive eruptions [e.g., Sable *et al.*, 2006, 2009, Arzilli *et al.*, 2019, Bamber *et al.*, 2020]. The pantelleritic magmas may favour highly explosive eruptions reaching viscosity of 10^6 Pa·s even with a low crystallinity at ≤ 750 °C (Figure 5). Therefore, the tendency of such magmas to fragment brittle or to flow effusively may be strongly controlled by temperature (Figure 5) and/or rapid decompression and strain localization, as suggested by Hughes *et al.* [2017]. Another process that should be considered is the crystallization of nanolites during fast perturbation of undercooling [Mujin and Nakamura, 2014, Di Genova *et al.*, 2020]. Nanolites may form during fast magma ascent in iron-rich peralkaline rhyolitic magmas, and their formation could change the magma viscosity by several orders of magnitude [Di Genova *et al.*, 2020]. All these hypotheses indicate that the complexity of pantellerite eruptive phenomena should be further investigated with more experimental and modelling studies to better understand the fragmentation process and the highly explosive eruptions in peralkaline rhyolitic systems.

Acknowledgements

This research has been supported by PRIN2017 (2017J277S9-MC). We thank John C. White and the other anonymous reviewer for their contribution to the review of this work and useful comments that helped us to improve this manuscript.

References

- Aiuppa, A., Franco, A., Von Glasow, R., Allen, A. G., D'Alessandro, W., Mather, T. A., Pyle, D. M., and Valenza, M. (2007). The tropospheric processing of acidic gases and hydrogen sulphide in volcanic gas plumes as inferred from field and model investigations. *Atmos. Chem. Phys.*, 7, 1441–1450.
- Arzilli, F. and Carroll, M. R. (2013). Crystallisation kinetics of alkali feldspars in cooling and decompression-induced crystallisation experiments in trachytic melt. *Contrib. Mineral. Petrol.*, 166, 1011–1027.
- Arzilli, F. *et al.* (2019). Magma fragmentation in highly explosive basaltic eruptions induced by rapid crystallization. *Nat. Geosci.*, 12, 1023–1028.
- Arzilli, F., Fabbriozio, A., Schmidt, M. W., Petrelli, M., Maimaiti, M., Dingwell, D. B., Paris, E., Burton, M., and Carroll, M. R. (2018). The effect of diffusive re-equilibration time on trace element partitioning between alkali feldspar and trachytic melts. *Chem. Geol.*, 495, 50–66.
- Arzilli, F., Piochi, M., Mormone, A., Agostini, C., and Carroll, M. R. (2016). Constraining pre-eruptive magma conditions and unrest timescales during the Monte Nuovo eruption (1538 AD; Campi Flegrei, Southern Italy): integrating textural and CSD results from experimental and natural trachyphonolites. *Bull. Volcanol.*, 78, 1–20.
- Arzilli, F., Stabile, P., Fabbriozio, A., Landi, P., Scaillet, B., Paris, E., and Carroll, M. R. (2020). Crystallization kinetics of alkali feldspar in peralkaline rhyolitic melts: implications for pantelleria volcano. *Front. Earth Sci.*, 8, article no. 177.
- Avanzinelli, R. (2004). Crystallisation and genesis of peralkaline magmas from Pantelleria Volcano, Italy: an integrated petrological and crystal-chemical study. *Lithos*, 73, 41–69.
- Bailey, D. K. and MacDonald, R. (1987). Dry peralkaline felsic liquids and carbon dioxide flux through the Kenya rift zone. In Mysen, B., editor, *Magmatic Processes: Physicochemical Principles*, volume 1, pages 91–105. Geochemical Society, University Park, PA.
- Bamber, E. C., Arzilli, F., Polacci, M., Hartley, M. E., Fellowes, J., Di Genova, D., Chavarría, D., Saballos, J. A., and Burton, M. R. (2020). Pre- and syn-eruptive conditions of a basaltic Plinian eruption at Masaya Volcano, Nicaragua: the Masaya Triple

- Layer (2.1 ka). *J. Volcanol. Geotherm. Res.*, 392, article no. 106761.
- Barclay, J., Carroll, M. R., Houghton, B. F., and Wilson, C. J. N. (1996). Pre-eruptive volatile content and degassing history of an evolving peralkaline volcano. *J. Volcanol. Geotherm. Res.*, 74, 75–87.
- Barclay, J., Rutherford, M. J., Carroll, M. R., Murphy, M. D., Devine, J. D., Gardner, J., and Sparks, R. S. J. (1998). Experimental phase equilibria constraints on pre-eruptive storage conditions of the Soufriere Hills magma. *Geophys. Res. Lett.*, 25, 3437–3440.
- Bohrson, W. A. and Reid, M. R. (1997). Genesis of silicic peralkaline volcanic rocks in an ocean island setting by crustal melting and open-system processes: Socorro Island, Mexico. *J. Petrol.*, 38, 1137–1166.
- Brugger, C. R. and Hammer, J. E. (2010). Crystallisation kinetics in continuous decompression experiments: implications for interpreting natural magma ascent processes. *J. Petrol.*, 51, 1941–1965.
- Campagnola, S., Romano, C., Mastin, L., and Vona, A. (2016). Confort 15 model of conduit dynamics: applications to Pantelleria Green Tuff and Etna 122 BC eruptions. *Contrib. Mineral. Petrol.*, 171, 1–25.
- Cashman, K. V. (2004). Volatile controls on magma ascent and eruption. In Sparks, R. S. J. and Hawkesworth, C. J., editors, *The State of the Planet: Frontiers and Challenge in Geophysics*, pages 109–124. American Geophysical Union.
- Civetta, L., Cornette, Y., Crisci, G., Gillot, P. Y., Orsi, G., and Requejo, C. S. (1984). Geology, geochronology and chemical evolution of the island of Pantelleria. *Geol. Mag.*, 121, 541–562.
- Civetta, L., Cornette, Y., Gillot, P.-Y., and Orsi, G. (1988). The eruptive history of Pantelleria (Sicily Channel) in the last 50 ka. *Bull. Volcanol.*, 50, 47–57.
- Civetta, L., D'Antonio, M., Orsi, G., and Tilton, G. R. (1998). The geochemistry of volcanic rocks from Pantelleria island, Sicily channel: petrogenesis and characteristics of the mantle source region. *J. Petrol.*, 39, 1453–1491.
- Civile, D., Lodolo, E., Torterici, L., Lanzafame, G., and Brancolini, G. (2008). Relationships between magmatism and tectonics in a continental rift: the Pantelleria Island region (Sicily Channel, Italy). *Mar. Geol.*, 251, 32–46.
- Cottrell, E., Gardner, J. E., and Rutherford, M. J. (1999). Petrologic and experimental evidence for the movement and heating of the pre-eruptive Mi-noan rhyodacite (Santorini, Greece). *Contrib. Mineral. Petrol.*, 135, 315–331.
- Couch, S., Sparks, R. S. J., and Carroll, M. R. (2003). The kinetics of degassing - induced crystallisation at Soufriere Hills volcano, Montserrat. *J. Petrol.*, 44, 1477–1502.
- Di Carlo, I., Rotolo, S. G., Scaillet, B., Buccheri, V., and Pichavant, M. (2010). Phase equilibrium constraints on pre-eruptive conditions of recent felsic explosive volcanism at Pantelleria Island, Italy. *J. Petrol.*, 5, 2245–2276.
- Di Genova, D., Brooker, R. A., Mader, H. M., Drewitt, J. W., Longo, A., Deubener, J., Neuville, D. R., Fanara, S., Shebanova, O., Anzellini, S., and Arzilli, F. (2020). In situ observation of nanolite growth in volcanic melt: a driving force for explosive eruptions. *Sci. Adv.*, 6(39), article no. eabb0413.
- Di Genova, D., Romano, C., Hess, K.-U., Vona, A., Poe, B. T., Giordano, D., Dingwell, D., and Behrens, H. (2013). The rheology of peralkaline rhyolites from Pantelleria Island. *J. Volcanol. Geotherm. Res.*, 249, 201–216.
- Di Genova, D., Vasseur, J., Hess, K. U., Neuville, D. R., and Dingwell, D. B. (2017). Effect of oxygen fugacity on the glass transition, viscosity and structure of silica- and iron-rich magmatic melts. *J. Non. Cryst. Solids*, 470, 78–85.
- Duffield, W. A. (1990). Eruptive fountains of silicic magma and their possible effects on tin content of fountain-fed lavas. *Geol. Soc. Am. Spec. Pap.*, 246, 251–261.
- Edmonds, M., McGee, K. A., and Doukas, M. P. (2008). Chlorine degassing during the lava dome-building eruption of Mount St. Helens 2004–2005. In Sherrod, D. R., Scott, W. E., and Stauffer, P. H., editors, *A Volcano Rekindled: The Renewed Eruption of Mount St. Helens 2004–2006*, volume 1750, pages 573–589. U.S. Geological Survey Professional Paper. Chap. 27.
- Gardner, J. E., Carey, S., Rutherford, M., and Sigurdson, H. (1995). Petrologic diversity of Mount St. Helens dacites during the last 4000 years: implications for magma mixing. *Contrib. Mineral. Petrol.*, 119, 224–238.
- Geschwind, C.-H. and Rutherford, M. J. (1992). Cumingtonite and the evolution of the Mount St. Helens (Washington) magma system: an experimental study. *Geology*, 20, 1011–1014.

- Ghiorso, M. S. and Gualda, G. A. R. (2015). An H₂O–CO₂ mixed fluid saturation model compatible with rhyolite-MELTS. *Contrib. Mineral. Petrol.*, 169, article no. 53.
- Gioncada, A. and Landi, P. (2010). The pre-eruptive volatile contents of recent basaltic and pantelleritic magmas at Pantelleria (Italy). *J. Volcanol. Geotherm. Res.*, 189, 191–201.
- Giordano, D., Russell, J. K., and Dingwell, D. B. (2008). Viscosity of magmatic liquids: a Model. *Earth Planet. Sci. Lett.*, 271, 123–134.
- Gottsmann, J. and Dingwell, D. B. (2002). The thermal history of a spatter-fed lava flow: the 8-ka pantellerite flow on Mayor Island, New Zealand. *Bull. Volcanol.*, 64, 410–422.
- Gualda, G. A. R., Ghiorso, M. S., Lemons, R. V., and Carley, T. L. (2012). Rhyolite- MELTS: a modified calibration of MELTS optimized for silica-rich, fluid-bearing magmatic systems. *J. Petrol.*, 53, 875–890.
- Hammer, J. E. (2004). Crystal nucleation in hydrous rhyolite: Experimental data applied to classical theory. *Am. Mineral.*, 89, 1673–1679.
- Hammer, J. E. (2006). Influence of *f*O₂ and cooling rate on the kinetics and energetics of Fe-rich basalt crystallization. *Earth Planet. Sci. Lett.*, 248, 618–637.
- Horn, S. and Smincke, H. U. (2000). Volatile emission during the eruption of Baitoushan volcano (China/North Korea) ca. 969 AD. *Bull. Volcanol.*, 61, 537–555.
- Houghton, B. F., Weaver, S. D., Wilson, C. J. N., and Lanphere, M. A. (1992). Evolution of a quaternary peralkaline volcano: Major Island, New Zealand. *J. Volcanol. Geotherm. Res.*, 51, 217–236.
- Hughes, E. C., Neave, D. A., Dobson, K. J., Withers, P. J., and Edmonds, M. (2017). How to fragment peralkaline rhyolites: Observations on pumice using combined multi-scale 2D and 3D imaging. *J. Volcanol. Geotherm. Res.*, 336, 179–191.
- Huppert, H. E. and Woods, A. W. (2002). The role of volatiles in magma chamber dynamics. *Nature*, 420, 493–495.
- Iddon, F., Jackson, C., Hutchison, W., Fontijn, K., Pyle, D. M., Mather, T. A., Yirgu, G., and Edmonds, M. (2018). Mixing and crystal scavenging in the Main Ethiopian Rift revealed by trace element systematics in feldspars and glasses. *Geochem. Geophys. Geosyst.*, 20, 1–30.
- Jeffery, A., J. and Gertisser, R. (2018). Peralkaline felsic magmatism of the Atlantic Islands. *Front. Earth Sci.*, 6, article no. 145.
- Jordan, N. J., John, C., White, R. M., and Rotolo, S. G. (2021). Evolution of the magma system of Pantelleria (Italy) from 190 ka to present. *C. R. Géosci.*, pages 1–17. Online first (2021), <https://doi.org/10.5802/crgeos.50>.
- Jordan, N. J., Rotolo, S. G., Williams, R., Speranza, F., McIntosh, W. C., Branney, M. J., and Scaillet, S. (2018). Explosive eruptive history of Pantelleria, Italy: Repeated caldera collapse and ignimbrite emplacement at a peralkaline volcano. *J. Volcanol. Geotherm. Res.*, 349, 47–73.
- Kovalenko, V. I., Herving, R. L., and Sheridan, M. F. (1988). Ion-microprobe analyses of trace elements in anorthoclase, hedembergite, aenigmatite, quartz, apatite and glass in Pantellerite: evidence for high water content in pantellerite melt. *Am. Miner.*, 73, 1038–1045.
- La Spina, G., Arzilli, F., Llewellyn, E. W., Burton, M. R., Clarke, A. B., Vitturi, M. D. M., Polacci, M., Hartley, M. E., Di Genova, D., and Mader, H. M. (2021). Explosivity of basaltic lava fountains is controlled by magma rheology, ascent rate and outgassing. *Earth Planet. Sci. Lett.*, 553, article no. 116658.
- Landi, P. and Rotolo, S. G. (2015). Cooling and crystallization recorded in trachytic enclaves hosted in pantelleritic magmas (Pantelleria, Italy): implications for pantellerite petrogenesis. *J. Volcanol. Geotherm. Res.*, 301, 169–179.
- Lanzo, G., Landi, P., and Rotolo, S. G. (2013). Volatiles in pantellerite magmas: a case study of the Green Tu Plinian eruption (Island of Pantelleria, Italy). *J. Volcanol. Geotherm. Res.*, 262, 153–163.
- Le Maitre, R. W., editor (2002). *Igneous Rocks, a Classification and Glossary of Terms: Recommendations of the International Union of Geological Sciences Subcommission on the Systematics of Igneous Rocks*. Cambridge University Press, Cambridge, UK, 2nd edition. 236 p.
- Liszewska, K., White, J., MacDonald, R., and Bagiński, B. (2018). Compositional and thermodynamic variability in a stratified magma chamber: evidence from the Green Tuff ignimbrite (Pantelleria, Italy). *J. Petrol.*, 59, 2245–2272.
- Lowestern, J. B. and Mahood, G. A. (1991). New data on magmatic H₂O contents with implications for petrogenesis and eruptive dynamics at Pantelleria.

- Bull. Volcanol.*, 54, 78–83.
- MacDonald, R. (1974). Nomenclature and petrochemistry of the peralkaline oversaturated extrusive rocks. *Bull. Volcanol.*, 38, 498–516.
- MacDonald, R., Bagiński, B., Belkin, H. E., Dzierzanowski, P., and Ježak, L. (2008). Compositional variations in apatites from a benmoreite-peralkaline rhyolite volcanic suite, Kenya Rift Valley. *Mineral. Mag.*, 72, 1147–1161.
- MacDonald, R., Bagiński, B., Leat, P. T., White, J. C., and Dzierzanowski, P. (2011). Mineral stability in peralkaline silicic rocks: information from trachytes of the Menengai volcano, Kenya. *Lithos*, 125, 553–568.
- Mader, H. M., Llewellyn, E. W., and Müller, S. P. (2013). The rheology of two-phase magmas: a review and analysis. *J. Volcanol. Geotherm. Res.*, 257, 135–158.
- Mahood, G. A. and Hildreth, W. (1986). Geology of the peralkaline volcano at Pantelleria, Strait of Sicily. *Bull. Volcanol.*, 48, 143–172.
- Marshall, A. S., MacDonald, R., Rogers, N. W., Fitton, J. G., Tindle, A. G., Nejbert, K., and Hinton, R. W. (2009). Fractionation of peralkaline silicic magmas: the greater Olkaria volcanic complex, Kenya Rift Valley. *J. Petrol.*, 50, 323–359.
- Martel, C. (2012). Eruption dynamics inferred from microlite crystallization experiments: application to Plinian and dome-forming eruptions of Mt Pelée (Martinique, Lesser Antilles). *J. Petrol.*, 53, 699–725.
- Martel, C. and Schmidt, B. C. (2003). Decompression experiments as an insight into ascent rates of silicic magmas. *Contrib. Mineral. Petrol.*, 144, 397–415.
- Masotta, M., Pontesilli, A., Mollo, S., Armienti, P., Ubide, T., Nazzari, M., and Scarlato, P. (2020). The role of undercooling during clinopyroxene growth in trachybasaltic magmas: insights on landmagma decompression and cooling at Mt. Etna volcano. *Geochim. Cosmochim. Acta*, 268, 258–276.
- Mattia, M., Bonaccorso, A., and Guglielmino, F. (2007). Ground deformations in the Island of Pantelleria (Italy): insights into the dynamic of the current intereruptive period. *J. Geophys. Res.*, 112, article no. B11406.
- Mollard, E., Martel, C., and Bourdier, J. L. (2012). Decompression-induced Crystallisation in Hydrated Silica-rich Melts: empirical models of experimental plagioclase nucleation and growth kinetics. *J. Petrol.*, 53, 1743–1766.
- Moore, G., Vennemann, T., and Carmichael, I. S. E. (1998). An empirical model for the solubility of H₂O in magmas to 3 kilobars. *Am. Mineral.*, 83, 36–42.
- Mujin, M. and Nakamura, M. (2014). A nanolite record of eruption style transition. *Geology*, 42(7), 611–614.
- Mungall, J. E. and Martin, R. F. (1995). Petrogenesis of basalt–co-mendite and basalt–pantellerite suites, Terceira, Azores, and some implications for the origin of ocean-island rhyolites. *Contrib. Mineral. Petrol.*, 119, 43–55.
- Mysen, B. O. (2007). The solution behaviour of H₂O in peralkaline aluminosilicate melts at high pressure with implication for properties of hydrous melts. *Geochim. Cosmochim. Acta*, 71, 1820–1834.
- Mysen, B. O. and Toplis, M. J. (2007). Structural behaviour of Al³⁺ in peralkaline, metaluminous, and peraluminous silicate melts and glasses at ambient pressure. *Am. Mineral.*, 92, 933–946.
- Neave, D. A. (2020). Chemical variability in peralkaline magmas and magma reservoirs: insights from the Khaggiar lava flow, Pantelleria, Italy. *Contrib. Mineral. Petrol.*, 175, article no. 39.
- Neave, D. A., Fabbro, G., and Herd, R. (2012). Melting, differentiation and Degassing at the Pantelleria Volcano, Italy. *J. Petrol.*, 53, 637–663.
- Ni, H., Keppler, H., Walte, N., Schiavi, F., Chen, Y., Masotta, M., and Li, Z. (2014). *In situ* observation of crystal growth in a basalt melt and the development of crystal size distribution in igneous rocks. *Contrib. Mineral. Petrol.*, 167, article no. 1003.
- Orsi, G., Ruvo, L., and Scarpati, C. (1991). The recent explosive volcanism at Pantelleria. *Geol. Rundsch.*, 80, 187–200.
- Papale, P. (1999). Modelling of the solubility of H₂O + CO₂ fluid in silicate liquids. *Am. Mineral.*, 84, 477–792.
- Papale, P., Moretti, R., and Barbato, D. (2006). The compositional dependence of the saturation surface of H₂O + CO₂ fluids in silicate melts. *Chem. Geol.*, 229, 78–95.
- Papale, P. and Polacci, M. (1999). Role of carbon dioxide in the dynamics of magma ascent in explosive eruptions. *Bull. Volcanol.*, 60, article no. 583e594.
- Peccerillo, A., Barberio, M. R., Yirgu, G., Ayalew, D., Barbieri, M., and Wu, T. W. (2003). Relationships between Mafic and Peralkaline Silicic Magmatism in Continental Rift Settings: a Petrological, Geo-

- chemical and Isotopic Study of the Gedemsa Volcano, Central Ethiopian Rift. *J. Petrol.*, 44, 2003–2032.
- Polacci, M. et al. (2018). Crystallisation in basaltic magmas revealed via *in situ* 4D synchrotron X-ray microtomography. *Sci. Rep.*, 8, article no. 8377.
- Pontesilli, A., Masotta, M., Nazzari, M., Mollo, S., Armienti, P., Scarlato, P., and Brenna, M. (2019). Crystallization kinetics of clinopyroxene and titanomagnetite growing from a trachybasaltic melt: New insights from isothermal time-series experiments. *Chem. Geol.*, 510, 113–129.
- Prosperini, N., Perugini, D., Poli, G., and Manetti, P. (2000). Magmatic enclaves distribution within the Khaggiar lava dome (Pantelleria, Italy): implication for magma chamber dynamics and eruption. *Acta Vulcanol.*, 12, 37–47.
- Ren, M., Omenda, P. A., Anthony, E. Y., White, J. C., MacDonald, R., and Bailey, D. K. (2006). Application of the QUILF thermobarometer to the peralkaline trachytes and pantellerites of the Eburre volcanic complex, East African Rift, Kenya. *Lithos*, 91, 109–124.
- Roggensack, K., Hervig, R. L., McKnight, S. B., and Williams, S. N. (1997). Explosive basaltic volcanism from Cerro Negro volcano: Influence of volatiles on eruptive style. *Science*, 277, 1639–1642.
- Romano, P., Andújar, J., Scaillet, B., Romengo, N., Di Carlo, I., and Rotolo, S. G. (2018). Phase equilibria of Pantelleria trachytes (Italy): constraints on pre-eruptive conditions and on the metaluminous to peralkaline transition in silicic magmas. *J. Petrol.*, 59, 559–588.
- Romano, P., Di Carlo, I., Andújar, J., and Rotolo, S. G. (2021). Water solubility in trachytic and pantelleritic melts: an experimental study. *C. R. Géosci.* this issue.
- Romano, P., Scaillet, B., White, J. C., Andújar, J., Di Carlo, I., and Rotolo, S. G. (2020). Experimental and thermodynamic constraints on mineral equilibrium in pantelleritic magmas. *Lithos*, 376–377, article no. 105793. 22 p.
- Romano, P., White, J. C., Ciulla, A., Di Carlo, I., D’Orlando, C., Landi, P., and Rotolo, S. G. (2019). Volatiles and trace elements content in melt inclusions from the zoned Green Tuff ignimbrite (Pantelleria, Sicily): petrological inferences. *Ann. Geophys.*, 62(1), article no. VO09.
- Romengo, N., Landi, P., and Rotolo, S. G. (2012). Evidence of basaltic magma intrusions in a trachytic magma chamber at Pantelleria (Italy). *Period. Mineral.*, 81, 163–178.
- Ronga, F., Lustrino, M., Marzoli, A., and Melluso, L. (2009). Petrogenesis of a basalt-comendite-pantellerite rock suite: the Boseti volcanic complex (main Ethiopian rift). *Mineral. Petrol.*, 98, 227–243.
- Rotolo, S. G., Agnesi, V., Conoscenti, C., and Lanzo, G. (2017). Pantelleria Island (Strait of Sicily): Volcanic history and geomorphological landscape. In Soldati, M. and Marchetti, M., editors, *Landscapes and Landforms of Italy*, World Geomorphological Landscapes. Springer, Cham.
- Rotolo, S. G., La Felice, S., Mangalaviti, A., and Landi, P. (2007). Geology and petrochemistry of the recent (<25 ka) silicic volcanism at Pantelleria Island. *Boll. Soc. Geol. It.*, 126, 191–208.
- Rotolo, S. G., Scaillet, S., La Felice, S., and Vita-Scaillet, G. (2013). A revision of the structure and stratigraphy of pre-Green Tuff ignimbrites at Pantelleria (Strait of Sicily). *J. Volcanol. Geotherm. Res.*, 250, 61–74.
- Rotolo, S. G., Scaillet, S., Speranza, F., White, J. C., Williams, R., and Jordan, N. J. (2021). Volcanological evolution of Pantelleria Island (Strait of Sicily) peralkaline volcano: a review. *C. R. Géosci.*, pages 1–22. Online first (2021), <https://doi.org/10.5802/crgeos.51>.
- Rutherford, M. J. and Devine, J. D. (1996). Pre-eruption pressure–temperature conditions and volatiles in the 1991 dacitic magma of Mount Pinatubo. In Newhall, C. G. and Punongbayan, R. S., editors, *Fire and Mud: Eruptions and Lahars of Mount Pinatubo, Philippines*, pages 751–766. PHIVOLCS and University of Washington Press, Seattle.
- Rutherford, M. J., Sigurdsson, H., Carey, S., and Davis, A. (1985). The May 18, 1980, eruption of Mount St. Helens 1. Melts composition and experimental phase equilibria. *J. Geophys. Res.*, 90, 2929–2947.
- Sable, J. E., Houghton, B., Wilson, C. J. N., and Carey, R. J. (2009). Eruption mechanisms during the climax of the Tarawera 1886 basaltic Plinian eruption inferred from microtextural. In *Studies in Volcanology: The Legacy of George Walker*, volume 2, page 129.
- Sable, J. E., Houghton, B. F., Del Carlo, P., and Coltelli, M. (2006). Changing conditions of magma ascent and fragmentation during the Etna 122 BC

- basaltic Plinian eruption: Evidence from clast microtextures. *J. Volcanol. Geotherm. Res.*, 158(3-4), 333–354.
- Scaillet, B. and MacDonald, R. (2001). Phase Relations of peralkaline silicic magmas and petrogenetic implications. *J. Petrol.*, 42, 825–845.
- Scaillet, B. and MacDonald, R. (2003). Experimental constraints on the relationships between Peralkaline Rhyolites of the Kenya Rift Valley. *J. Petrol.*, 44, 1867–1894.
- Scaillet, B. and MacDonald, R. (2006). Experimental constraints on pre-eruption conditions of pantelleritic magmas: evidence from the Eburru complex, Kenya Rift. *Lithos*, 91, 95–108.
- Scaillet, S., Rotolo, S. G., La Felice, S., and Vita-Scaillet, G. (2011). High-resolution $^{40}\text{Ar}/^{39}\text{Ar}$ chronostratigraphy of the post-caldera (<20 ka) volcanic activity at Pantelleria, Sicily Strait. *Earth Planet. Sci. Lett.*, 309, 280–290.
- Scaillet, S., Vita-Scaillet, G., and Rotolo, S. G. (2013). Millennial-scale phase relationships between ice-core and Mediterranean marine records: insights from high-precision $^{40}\text{Ar}/^{39}\text{Ar}$ dating of the Green Tuff of Pantelleria, Sicily Strait. *Quat. Sci. Rev.*, 78, 141–154.
- Schmidt, B. and Behrens, H. (2008). Water solubility in phonolite melts: Influence of melt composition and temperature. *Chem. Geol.*, 256, 259–268.
- Schmincke, H.-U. (1974). Volcanological aspects of peralkaline silicic welded ash-flow tuffs. *Bull. Volcanol.*, 38, 594–636.
- Shea, T. and Hammer, J. E. (2013). Kinetics of cooling- and decompression-induced crystallization in hydrous mafic-intermediate magmas. *J. Volcanol. Geotherm. Res.*, 260, 127–145.
- Sparks, R. S. J. (1978). The dynamics of bubble formation and growth in magmas: a review and analysis. *J. Volcanol. Geotherm. Res.*, 3, 1–37.
- Sparks, S. R. J. (2003). Dynamics of magma degassing. *Geol. Soc. Lond., Spec. Pub.*, 213, 5–22.
- Speranza, F., Landi, P., Caracciolo, F. D. A., and Pignatelli, A. (2010). Paleomagnetic dating of the most recent silicic eruptive activity at Pantelleria (Strait of Sicily). *Bull. Volcanol.*, 72, 847–858.
- Stabile, P., Appiah, E., Bello, M., Giuli, G., Paris, E., and Carroll, M. R. (2020). New IR spectroscopic data for determination of water abundances in hydrous pantelleritic glasses. *Am. Mineral.*, 105(7), 1060–1068.
- Stabile, P. and Carroll, M. R. (2020). Petrologic experimental data on Vesuvius and Campi Flegrei magmatism: a review. In De Vivo, B., Belkin, H. E., and Rolandi, G., editors, *Vesuvius, Campi Flegrei, and Campanian Volcanism*, pages 323–369. Elsevier. ISBN 9780128164549.
- Stabile, P., Giuli, G., Cicconi, M. R., Paris, E., Trapananti, A., and Behrens, H. (2017). The effect of oxygen fugacity and Na/(Na+K) ratio on iron speciation in pantelleritic glasses. *J. Non-Cryst. Solids*, 478, 65–74.
- Stabile, P., Radica, E., Bello, M., Behrens, H., Carroll, M. R., Paris, E., and Giuli, G. (2018). H₂O solubility in pantelleritic melts: pressure and alkali effects. *N. Jb. Miner. Abh.*, 195, 1–9.
- Stabile, P., Sicola, S., Giuli, G., Paris, E., Carroll, M. R., Deubener, J., and Di Genova, D. (2021). The effect of iron and alkali on the nanocrystal-free viscosity of volcanic melts: A combined Raman spectroscopy and DSC study. *Chem. Geol.*, 559, article no. 119991.
- Stabile, P., Webb, S., Knipping, J. K., Behrens, H., Paris, E., and Giuli, G. (2016). Viscosity of pantelleritic and alkali-silicate melts: effect of Fe redox state and Na/(Na + K) ratio. *Chem. Geol.*, 422, 73–82.
- Stevenson, R. J., Bagdassarov, N. S., Dingwell, D. B., and Romano, C. (1998). The influence of trace amounts of water on the viscosity of rhyolites. *Bull. Volcanol.*, 60, 89–97.
- Stevenson, R. J., Briggs, R. M., and Hodder, A. P. W. (1993). Emplacement history of a low-viscosity, fountain-fed pantelleritic lava flow. *J. Volcanol. Geotherm. Res.*, 57, 39–56.
- Stevenson, R. J. and Wilson, L. (1997). Physical volcanology and eruption dynamics of peralkaline agglutinates from Pantelleria. *J. Volcanol. Geotherm. Res.*, 79, 97–122.
- Stock, M. J., Humphreys, M. C. S., Smith, V. C., Isaia, R., Brooker, R. A., and Pyle, D. M. (2018). Tracking volatile behaviour in sub-volcanic plumbing systems using apatite and glass: Insights into pre-eruptive processes at Campi Flegrei, Italy. *J. Petrol.*, 59(12), 2463–2492.
- Vona, A., Romano, C., Dingwell, D. B., and Giordano, D. (2011). The rheology of crystal-bearing basaltic magmas from Stromboli and Etna. *Geochim. Cosmochim. Acta*, 75, 3214–3236.
- Webster, J. D., Taylor, R. P., and Bean, C. (1993). Pre-eruptive melt composition and constraints on de-

- gassing of a water-rich pantellerite magma, Fantale volcano, Ethiopia. *Contrib. Mineral. Petrol.*, 114, 53–62.
- White, J. C., Parker, D. F., and Ren, M. (2009). The origin of trachyte and pantellerite from Pantelleria, Italy: insights from major elements, trace elements, and thermodynamic modelling. *J. Volcanol. Geotherm. Res.*, 179, 33–55.
- White, J. C., Ren, M., and Parker, D. F. (2005). Variation in mineralogy, temperature, and oxygen fugacity in a suite of strongly peralkaline lavas and tuffs, Pantelleria, Italy. *Canad. Mineral.*, 43, 1331–1347.
- Wilding, M. C., MacDonald, R., Davies, J. E., and Fallick, A. E. (1993). Volatile characteristics of peralkaline rhyolites from Kenya: an ion microprobe, infrared spectroscopic and hydrogen isotope study. *Contrib. Mineral. Petrol.*, 114, 264–275.
- Williams, R. (2010). *Emplacement of Radial Pyroclastic Density Currents Over Irregular Topography: The chemically-zoned, low aspect-ratio Green Tuff ignimbrite, Pantelleria, Italy*. PhD thesis, University of Leicester, Leicester, UK. 224 p., <https://doi.org/10.6084/m9.figshare.789054>.
- Williams, R., Branney, M. J., and Barry, T. L. (2014). Temporal and spatial evolution of a waxing then waning catastrophic density current revealed by chemical mapping. *Geology*, 42, 107–110.